

FLUXES AND GRADIENTS IN THE CONVECTIVE SURFACE LAYER AND THE POSSIBLE ROLE OF BOUNDARY-LAYER DEPTH AND ENTRAINMENT FLUX

G. J. STEENEVELD*, A. A. M. HOLTSLAG and H. A. R. DEBRUIN
*Meteorology and Air Quality, Wageningen University, Duivendaal 2, 6701 AP Wageningen,
The Netherlands*

(Received in final form 2 June 2004)

Abstract. We study the relation between fluxes and gradients in the very unstable surface layer by comparing recent proposals in the literature with the well-known Businger–Dyer functions. The recent proposals include results from large-eddy simulation (LES), which account for entrainment effects and effects of the boundary-layer depth. A comparison of the relationships is made with experimental data. The LES-based gradient functions show the impact of entrainment in the surface layer, but the scatter in the field data is too large to confirm this. Therefore this result is preliminary and future tests against new observations are recommended. It appears that the Businger–Dyer relationship behaves differently to the alternatives, and that it deviates from observations for large stability.

Keywords: Entrainment, Free convection, Similarity theory, Surface-layer gradient functions.

1. Introduction

Businger et al. (1971) published their famous flux–profile relationships based on turbulent flux and vertical profile observations above prairie grassland over horizontal homogeneous terrain in Kansas, U.S.A. After some adaptations, these relationships are now known as the Businger–Dyer relations (see Dyer, 1974; Businger, 1988; Högström, 1988, and for an heuristic derivation, Fleagle and Businger, 1980) that read as

$$\phi_h = \phi_m^2 = \left(1 - 16 \frac{z}{L}\right)^{-1/2} \quad (1)$$

in which ϕ_h and ϕ_m are dimensionless gradients of temperature and wind speed, z the height above the surface, and L the Obukhov length.

The Kansas experiment in 1968 was set up to verify the Monin–Obukhov similarity theory (MOST), a theory that is based on the assumption that in the atmospheric surface layer (ASL) z and L are the only relevant turbulent length scales. Consequently, according to MOST, the height of the convective boundary layer (CBL), h , does not play a role in the ASL (e.g. Holtslag and Nieuwstadt, 1986). Moreover, the Kansas dataset was confined to conditions

* E-mail: gert-jan.steeneveld@wur.nl

with $-z/L$ smaller than 1. For large values of $-z/L$, in particular in the so-called free convection region where the influence of friction velocity, u_* , is expected to vanish, there is still no unanimity in the literature on the flux-gradient relations. The Businger–Dyer relationships do not fulfill the relations found from similarity theory assuming that only the buoyancy flux (which is $\frac{\kappa}{\theta} \overline{w\theta}$ if humidity effects are ignored) and the actual height z are of relevance only.

There is a growing interest in the boundary-layer community to improve the widely used Equation (1) by accounting for additional phenomena. This is a challenging task owing to the scatter of most datasets. Recently, Halldin et al. (1999) and Johansson et al. (2001) found that ϕ_m depends on h/L . Panofsky et al. (1977) already found that the boundary-layer depth is a scaling parameter for the horizontal velocity variances under convective conditions in the surface layer.

In this study we will present additional arguments and evidence that h and the entrainment flux might be relevant in the ASL also. As such, flux–profile relations are derived for the surface layer by considering the implications of ideas presented in Cuijpers and Holtslag (1998, hereafter referred to as CH98) for the CBL (see also Holtslag, 1998). The objective of our study is to investigate whether the modified gradient formulations apply in the convective ASL. In addition, we compare these with surface-layer expressions. Data collected at the Cabauw tower in The Netherlands include profiles, fluxes, and the boundary-layer depth, and together with data from CASES-99 (e.g. Poulos et al., 2002) have been used to verify the various formulations. In addition, we will pay attention to conditions of free convection in the surface layer.

The paper is organised as follows. In Section 2 the theoretical background is presented. Section 3 contains the necessary information on the datasets including the energy budgets at the surface and through the boundary layer. The results are given in Section 4. Section 5 deals with the behaviour of gradient functions during local free convection, followed by a discussion in Section 6 and the conclusions in Section 7.

2. Theory

Large-eddy simulation (LES) has shown that vertical gradients in the CBL are well described by (e.g. Moeng and Wyngaard, 1989; hereafter MW89),

$$\frac{\partial \bar{X}}{\partial z} = \frac{\overline{w\chi_0}}{hw_*} f_1\left(\frac{z}{h}\right) + \frac{\overline{w\chi_{\text{entr}}}}{hw_*} f_2\left(\frac{z}{h}\right), \quad (2)$$

where f_1 and f_2 are gradient functions concerning bottom-up and top-down transport, respectively. Here X is a scalar such as potential temperature ($\bar{\theta}$),

specific humidity (\bar{q}) or a trace gas (\bar{C}). Furthermore, $\overline{w\chi_0}$ and $\overline{w\chi_{\text{entr}}}$ are the surface flux and entrainment flux (at the top of the CBL) of X respectively, and $w_* = \left(\frac{g}{\theta} \overline{w\theta_0} h\right)^{1/3}$, where h is the CBL depth.

According to MW89, Equation (2) is given by

$$\frac{\partial \bar{X}}{\partial z} = c_1 \frac{\overline{w\chi_0}}{w_* h} \left(\frac{z}{h}\right)^{-3/2} + c_2 \frac{\overline{w\chi_{\text{entr}}}}{w_* h} \left(1 - \frac{z}{h}\right)^{-2} \quad (3)$$

with $c_1 = -0.4$ and $c_2 = -0.7$. This relationship has been obtained from a LES model by applying top-down, bottom-up mixing assumptions. Note that originally $c_1 = -0.4$ in MW89, but it appears that with $c_1 = -0.45$ a better fit to their LES data, as well as to the observations used in our study, is achieved (in particular close to the surface).

Alternatively, CH98 studied non-local fluxes in the CBL in addition to gradient transport. Their results can be written for the purely convective case as

$$\frac{\partial \bar{X}}{\partial z} = \frac{\overline{w\chi_{\text{NL}}} - \overline{w\chi}}{K} = \frac{\overline{w\chi_0}}{hw_*} \left(\frac{0.89\gamma \left(\frac{1+\alpha}{2}\right)}{c_k \left(\frac{z}{h}\right)^{2/3} \left(1 - \beta \frac{z}{h}\right)} - \frac{1 + (\alpha - 1) \frac{z}{h}}{\left(\frac{z}{h}\right)^{4/3} \left(1 - \frac{z}{h}\right)^2} \right) \quad (4)$$

with α the entrainment ratio defined by $\alpha = \overline{w\theta_{\text{entr}}}/\overline{w\theta_0}$, K is the turbulent diffusion coefficient, c_k , γ and β are empirical coefficients, and $\overline{w\chi_{\text{NL}}}$ is the non-local turbulent heat flux. A derivation of (4) is given in the Appendix. Thus Equation (4) describes scalar gradients as functions of z/h and the entrainment ratio α . The main question now is: how does this relationship behave in the convective surface layer i.e. for $z/h \leq 0.1$?

To compare the $\bar{\theta}$ and \bar{q} gradients from (3) and (4) with other expressions in the surface layer, we focus on two formulae that satisfy the so-called free convective limit, and a modified ‘Businger’-type formula. The three surface-layer proposals are summarized below:

(a) DeBruin (1999, from now on referred to as DB99), revised a ‘heuristic’ model (Fleagle and Businger, 1980) and found:

$$\phi_x = \frac{\partial \bar{X}}{\partial z} \frac{kz}{X_*} = \left(1 - 3 \frac{z}{L}\right)^{2/3} \left(1 - 10 \frac{z}{L}\right)^{-1}. \quad (5)$$

In the free convection limit ($-z/L \rightarrow \infty$) this relation leads to

$$\frac{\partial \bar{X}}{\partial z} = \frac{C \overline{w\chi_0}}{z w_f}, \quad (6)$$

where $C = -0.706$ and w_f is the convective velocity scale in the surface layer defined as $w_f = \left(\frac{g}{\theta} \overline{w\theta_0} z\right)^{1/3}$.

(b) Recently Wilson (2001) proposed (based on a re-analysis of the Kansas experiment):

$$\phi_x = \frac{kz}{P_t X_*} \frac{\partial \bar{X}}{\partial z} = \left(1 + 7.86 \left(\frac{z}{|L|} \right)^{2/3} \right)^{-1/2} \quad (7)$$

in which P_t is the Prandtl number defined as $P_t = K_m/K_h$ and taken as 0.95. In the case of free convection, this leads to the same relation as (6) with $C = -1.15$. For $-z/L \rightarrow \infty$, (7) behaves similarly to ‘classical’ free convection expressions (see Lumley and Panofsky, 1964, pp. 108–110; Turner, 1979, pp. 133–136; Monin and Yaglom, 1981, Chapter 4; Kader and Yaglom, 1990).

(c) The Businger–Dyer relationship (see above): $\phi_h = (1 - 16 \frac{z}{L})^{-1/2}$. This does not obey the $-1/3$ law for the free convection limit, so u_* does not vanish and $\frac{\partial \bar{X}}{\partial z}$ remains a function of u_* when $-z/L \rightarrow \infty$. Businger et al. (1971), Businger (1973), Wyngaard (1973) and Schumann (1988) discussed this feature, and Schumann proposed that in the free convection region $u_{*eff} = \epsilon w_*$, with u_{*eff} the effective value of u_* during convection and $\epsilon \approx 0.1$ for typical roughness over land.

The idea that u_* does not vanish at low wind speeds has been recognised before by e.g. Wyngaard (1973) and Businger (1973): ‘Close to the surface during a short period compared to large-scale convection, but during a long period compared to the time it takes to develop a wind profile, the profiles must be approximately the same as for a large-scale mean wind, consequently there is shear production and a friction velocity may be defined’. For a recent discussion on this matter and observational evidence we refer to Mahrt et al. (2001). Application to models is discussed by Beljaars (1995) and others.

In this paper, our goal is to find out whether relationships (3) and (4) behave properly in the surface layer, and how they compare with the above mentioned ASL formulations (not containing h). The various approaches will be compared with experimental data. In addition we wish to assess the impact of the boundary-layer depth and the entrainment ratio α on the surface-layer parameterisations. Note that in the above we assumed that the von Kármán constant $\kappa = 0.4$. Alternative functions with different values for κ will not be treated here, but can be found in e.g. Stull (1988), Dyer (1974) and Högström (1988).

3. Datasets

3.1. CABAUW

It should be noted in advance that for the observational verification of either (3) or (4), surface fluxes, scalar profiles and boundary-layer heights are necessary. Datasets containing all this information are very scarce (e.g. Johansson et al., 2001).

Part of the current dataset has been taken from 2 to 5 of May 1995 (DOY = 122–125) at Cabauw (51.971° N, 4.927° E; 0.7 m below mean sea level), The Netherlands (Van Ulden and Wieringa, 1996). This dataset contains profiles of mean temperature and specific humidity from the 200-m mast, and boundary layer depth measured with a RASS profiler. Eddy covariance sensible and latent heat fluxes measured at 5-m height completed the dataset. From the synoptic station De Bilt radiosoundings were added.

The synoptic situation was characterised by a high-pressure region centred in Poland; later on, the centre moved towards Austria. The weather was generally fair and the sky was nearly clear, with patchy cirrus clouds present. The wind was south-easterly and moderate. At DOYs 124 and 125 the wind speed decreased and veered between south and south-westerly. In the afternoon a sea breeze appeared, but observations after the passage of a frontal zone have not been included herein.

The latent heat flux ($L_v E$, with L_v the latent heat of vaporization and E the turbulent moisture flux) is the largest consumer of the available energy, because of the large water availability at Cabauw, especially in spring (e.g. DeBruin and Holtslag, 1982). Note that $L_v E$ has peak values around 250 W m^{-2} , and is the reason that the sensible heat flux did not exceed 50 W m^{-2} . Note also that, in this dataset, the surface energy budget is not balanced (i.e. the sum of observed H and $L_v E$ is less than net radiation minus soil heat flux). The imbalance reaches up to 150 W m^{-2} during daytime (30% of the net radiation), though we did not attempt to account for this feature in the present study because of the many uncertainties that still exist (Oncley et al., 2002). H and $L_v E$ are thus directly taken from the eddy correlation observations.

3.2. CASES-99

For comparing flux gradient relationships for large $-z/L$ (Section 5), we also examine observations from the CASES-99 experimental campaign, because the surface layer was more unstable in CASES-99 than in the Cabauw dataset. Therefore, the surface sensible flux and the vertical temperature gradients were larger than at Cabauw, and as a consequence, the uncertainty in the observations is smaller. CASES-99 provides advantageous observations for testing surface layer similarity during free convection, although the experiment focused on stable atmospheric conditions in the boundary layer (Poulos et al., 2002).

The experimental period ranged from October 1 to 31, 1999 and was conducted near Leon, Kansas, U.S.A., (37.6486° N, 96.7351° W, 431 m a.s.l.). This area was chosen for its lack of obstacles, and relatively flat terrain, with a surface comprised mainly of prairie grasses, with a typical roughness length

of $z_0 = 0.03$ m and low soil moisture content. More detailed information is given in Poulos et al. (2002). The experiment included a heavily instrumented 60-m tower operated by the National Center for Atmospheric Research from which we extracted vertical temperature gradients.

Due to the low soil moisture content, surface sensible heat fluxes and vertical temperature gradients are larger than at Cabauw, which is an advantage for studies of convective conditions. Typical values for H are 200 and 60 W m^{-2} for $L_v E$ during daytime; the non-closure of the surface energy balance amounts typically to 50 W m^{-2} (12% of the net radiation). The drawback of the current dataset is that the boundary-layer depth was not available (to us) during daytime.

3.3. DATA PROCESSING

The scalar gradients are derived from the mast observations by a least square fit according to (see e.g. Oncley et al., 1996; Frenzen and Vogel, 2001; Johansson et al., 2001):

$$X(z) = A + B \ln(z) + C \ln^2(z) + D \ln^3(z). \quad (8)$$

This method is sensitive to (a) errors when data are missing, especially at higher levels (Oncley et al., 1996), and (b) to outliers when used for estimating differentials. Akima (1970) show that the first problem can be minimised with a more advanced mathematical approach; we used (8) for simplicity. Moreover, it might be possible that systematic errors can affect the calculated gradients, e.g. when the radiation error for temperature measurements depends on wind speed and therefore increases systematically with height.

4. Results

4.1. ESTIMATED GRADIENTS VERSUS CABAUW OBSERVATIONS

We bring together theory (Equation (4)) and observations from Cabauw in Figures 1a and 2a, and show the observed and estimated mean temperature and humidity gradients respectively. For Equation (3) these results are shown in Figures 1b and 2b. The entrainment rate ratio was set to -0.25 for heat and $+0.2$ for humidity, which were derived as typical values from the 1200 UTC (1400 local time) radiosoundings. These values are used for all the calculations below. It is seen that Equations (3) and (4) describe the observations well, both for potential temperature and humidity. For both quantities the bias is rather small and for humidity the scatter is smaller than for

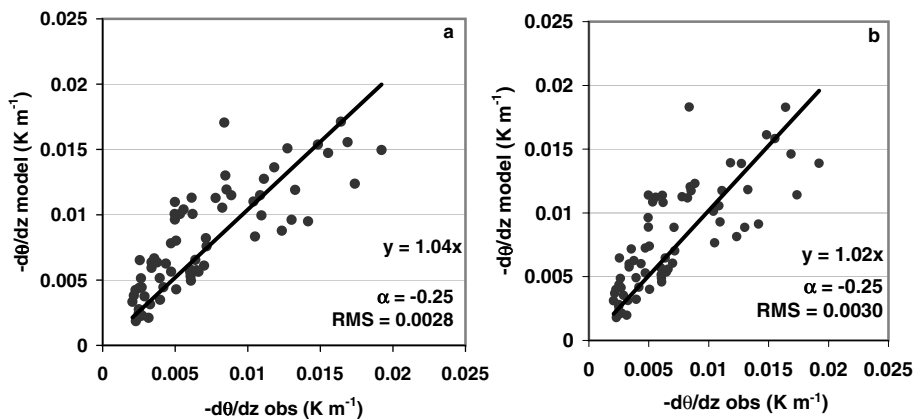


Figure 1. (a) Estimated versus observed mean temperature gradient in the convective surface layer at Cabauw for Equation (4). RMS represents the root-mean-square error between the model and the observations; (b), as in (a), but for Equation (3).

temperature. With the original model of MW89, (using $c_1 = -0.4$), we find an underestimate of 8% for heat and 2% for humidity, so indeed the use of $c_1 = -0.45$ is an improvement.

Although Equations (3) and (4) show equivalent skill on the current data, we may note that Equation (4) is more easily adapted to near-neutral conditions (including the u_* influence).

4.2. GRADIENT FUNCTIONS COMPARED TO ALTERNATIVE PROPOSALS

Using boundary-layer theory for the CBL, the scaling is (e.g. Holtslag and Nieuwstadt, 1986):

$$g_x = \frac{hw_*}{w\%_0} \left(\frac{-\partial\bar{X}}{\partial z} \right) \quad (9)$$

with the subscript of g_x given by $x = h$ for heat or $x = e$ for humidity and $\bar{X} = \bar{\theta}$ or \bar{q} . The dimensionless gradients are shown in Figures 3 and 4 as a function of z/h , together with the surface-layer alternatives and Cabauw observations. The data have been separated according to the atmospheric conditions: when $-z/L > 0.5$ and $-h/L > 5$ the data are represented by dots (convective, very unstable) and as triangles (weak convective).

At first we conclude that Equations (3) and (4) compare very well to the alternatives. Moreover, it is seen that DB99 agrees with the data quite well. Wilson's function shows a positive bias compared to the model and the other alternatives. Thus both $\bar{\theta}$ and \bar{q} show a good fit through the data, but the large data scatter prevents a clear preference for any of the models. Even the

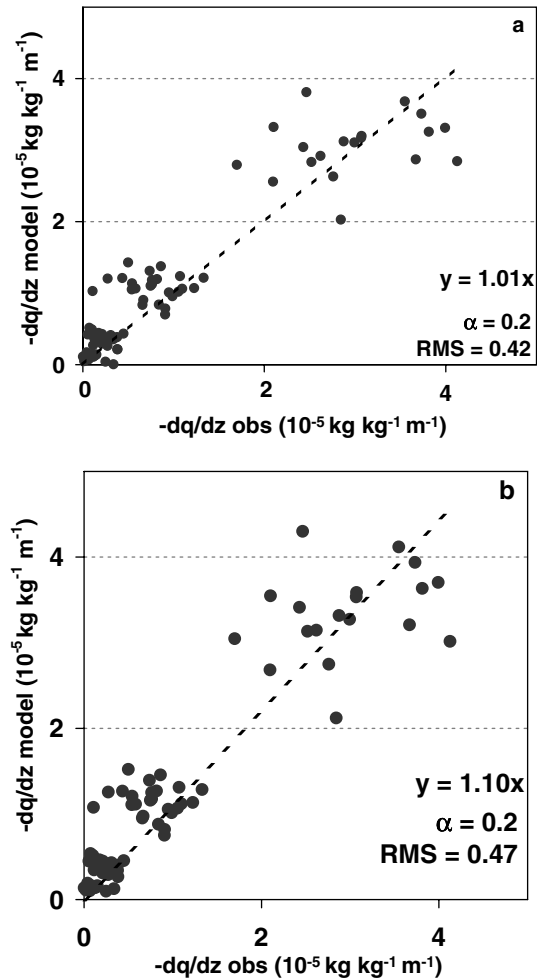


Figure 2. (a) Estimated versus observed mean humidity gradient in the convective surface layer at Cabauw; RMS represents the root-mean-square error between the model and the observations; (b), as in (a) but for Equation (3).

weak convective data (triangles in Figures 3 and 4) agree with the observations. Apparently, the influence of u_* can safely be neglected. Also the assumption $u_{*\text{eff}} = \varepsilon w_*$ (with $\varepsilon = 0.1$) performs rather well, although we found that the application of $\varepsilon = 0.22$ (not shown) results in the best fit through the data for $0.01 < z/h < 0.1$. With $\varepsilon = 0.22$ the curve is very close to the result of Equation (4) as well. As an illustration, Figure 5 shows $u_{*\text{eff}}$ versus w_* for the Cabauw dataset, and in this way we find $\varepsilon \cong 0.19$ (but the scatter is considerable).

Thus, here we present some evidence that the boundary-layer depth h is also a relevant variable in the surface layer for the gradient functions of heat

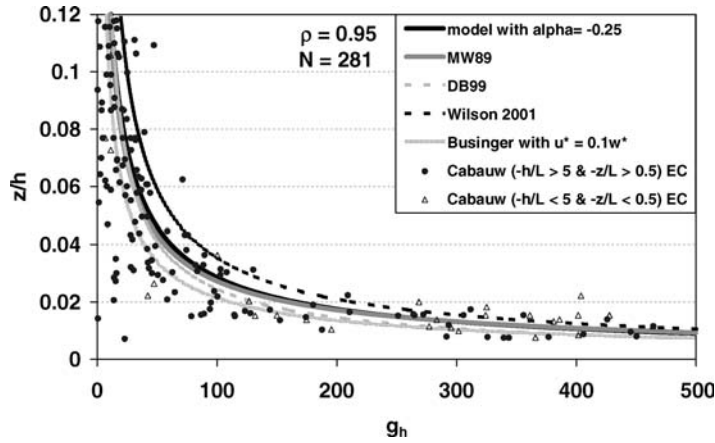


Figure 3. Gradient function (A8) for heat with alternatives and eddy correlation data. ((●) $-h/L > 5$ and $-z/L > 0.5$, (Δ) $-h/L < 5$ and $-z/L < 0.5$). ρ denotes the correlation coefficient between the model and observations.

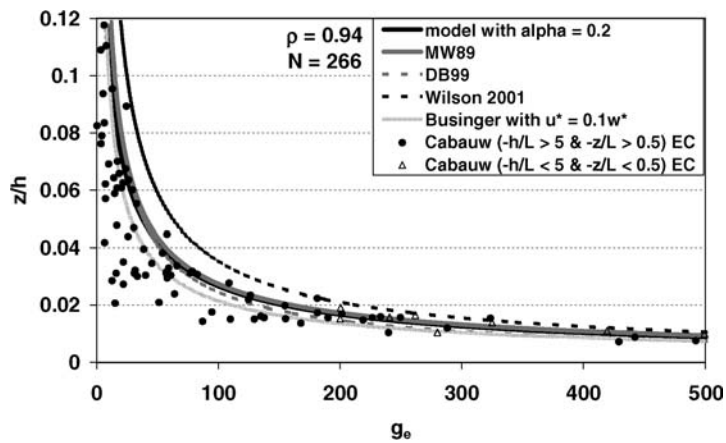


Figure 4. As Figure 3, but for specific humidity.

and moisture; recall that Halldin et al. (1999) and Johansson et al. (2001) also reported an h/L dependence in the gradient functions for the surface layer.

4.3. IMPACT OF ENTRAINMENT

Figure 6 shows the gradient relationship (4) for various values of the entrainment ratio α . A clear distinction between the curves is found, mainly at the top of the surface layer; near the surface the impact becomes smaller.

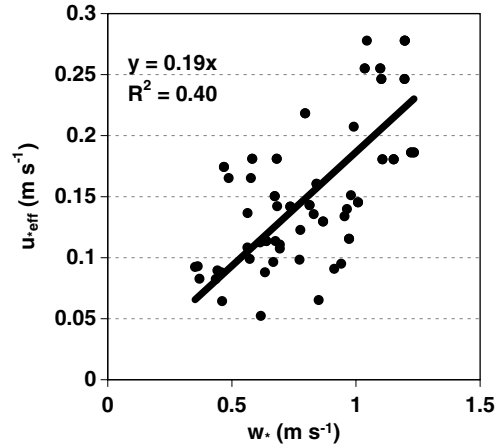


Figure 5. Scatter plot of observed u_{*eff} versus w_* at Cabauw.

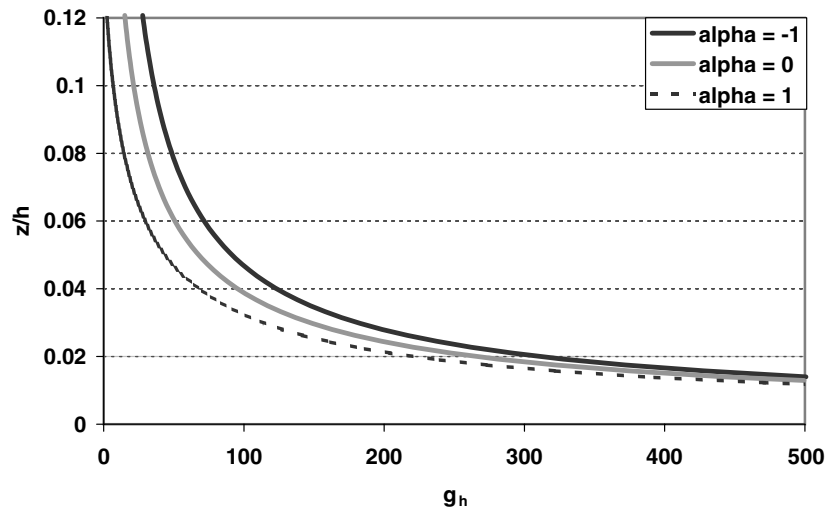


Figure 6. Gradient of mean potential temperature as a function of z/h and entrainment ratio α .

These LES-based functions show that the entrainment ratio affects both profiles of temperature and humidity in the surface layer. Unfortunately, because of the large scatter in the observations and because the estimation of the entrainment ratio is not a trivial point, confirmation with the field data is hard.

In addition, if entrainment rates are set to zero in Figures 1 and 2, the agreement is somewhat less for heat and somewhat better for humidity. So this cannot be seen as a definite test.

5. Flux–profile relationship under free convective conditions

From the viewpoint of MOST in the ASL, the turbulent regime at heights $z \gg |L|$ for a given u_* does not differ from the regime where z is fixed and not too great and u_* is small. This implies that the limiting case $-\frac{z}{L} \rightarrow \infty$ must be the same as $u_* \rightarrow 0$. Then similarity arguments lead to the feature that in this limit, the function J , defined by

$$J(\zeta) \equiv \frac{\overline{wT}_{fc}}{z^2 \sqrt{\frac{g}{\theta} \left| \frac{\partial \theta}{\partial z} \right|}^{3/2}} = \frac{k^2}{\phi_h^{3/2} \sqrt{|\zeta|}}, \tag{10}$$

approaches a constant. Here $\zeta = z/L$.

In order to show the main differences between these functions we plot in Figure 7 the expressions J as a function of ζ , using the ϕ_h functions of the original Businger–Dyer formulation (BD, Equation (1)), DeBruin (DB99, Equation (5)) and Wilson (W01, Equation (7)); observations are also shown. It is seen that the differences are insignificant for $-\zeta < 0.1$, but for $-\zeta > 1$ BD increases monotonically with $-\zeta$, whereas DB99 and W01 become constant respectively at 1.7 and 0.8. The DB99 curve has a minimum around $-\zeta$ equals 0.05. This shows that an appropriate test of the different ϕ_h functions is to use experimental data corresponding to $-\zeta > 1$.

Unfortunately, the scatter in our data is too large to be distinctive for this purpose. A plausible reason is that the temperature gradients are small for $-\zeta > 1$, so that J is difficult to determine accurately from profile and flux data.

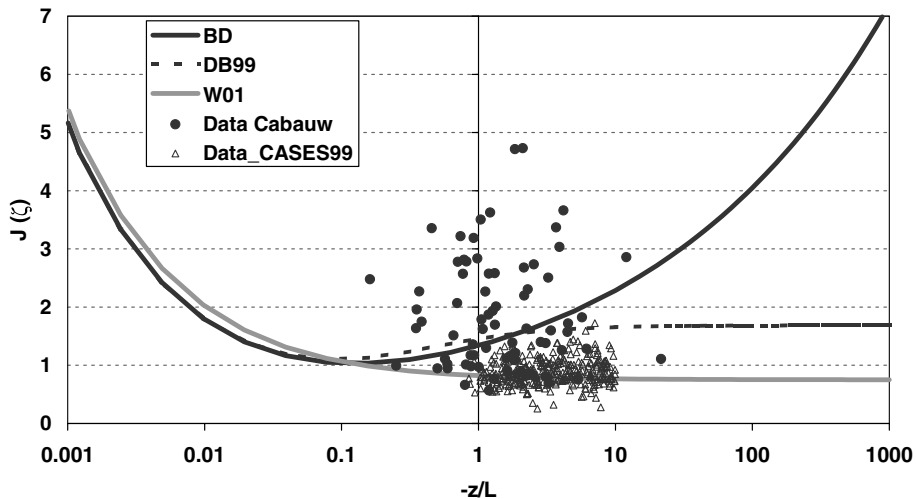


Figure 7. Flux–profile relationships as a function of z/L and observations from Cabauw and CASES-99 (the latter selected as $\partial\bar{\theta}/\partial z < -0.02 \text{ K m}^{-1}$).

In addition we have to be aware of statistical sampling problems, requiring long averaging times in very convective conditions. Nevertheless, the CASES-99 data (when selected for $\partial\bar{\theta}/\partial z < -0.02 \text{ K m}^{-1}$) appears to give the best fit for the W01 formulation. Because, observations of h were not available to us for this dataset, we are unable to investigate whether h plays a role here.

6. Discussion

6.1. SCALING

Wyngaard (1973) and Holtslag and Nieuwstadt (1986) suggest that, on the basis of similarity arguments, the relevant scaling variables in the ASL during free convection are $w\theta_0$, z and $\frac{g}{\theta}$. From these quantities the convective velocity scale w_f can be found. Then the most natural scaling for a convective ASL uses z and w_f ;

$$g_{xSL} = \frac{zw_f}{w\lambda_0} \left(-\frac{\partial\bar{X}}{\partial z} \right) \quad (11)$$

in which X is a scalar quantity. Thus g_{xSL} becomes a dimensionless scalar gradient. We found that such an approach leaves much more scatter than the scaling according to (9) (not shown), and (11) appears not to be suitable. On the other hand, the scatter in the current observations is so large that we have to be modest with proposing (9) as the definite way of scaling. Recall the relatively small surface fluxes and mean gradients in the current selection of the Cabauw dataset compared to those available during CASES-99, indicating large scatter in Figures 3 and 4.

6.2. SURFACE ENERGY BUDGET

At first sight, Figures 3 and 4 give excellent results in verifying Equation (4). On the other hand we must be aware of the non-closure of the surface energy budget. If the eddy correlation fluxes comprising the dataset of Section 3 are accurate, Figures 3 and 4 are indeed in good agreement with LES. Then the non-closure of the surface energy balance should be attributed to measurement problems in the net radiation or in the soil heat flux. However, this needs further investigation. On the other hand, if net radiation and soil heat flux are correct, then the surface heat fluxes must be adjusted, and the current findings need revision (see also the recent work by Rao, 2004).

7. Conclusions and recommendations

It is shown that descriptions for scalar gradient relationships, based on LES for the CBL, do relatively well for the surface layer. This is the case when the velocity scale w_* , the surface flux $\overline{w\chi}_0$ and the boundary-layer height h are used for scaling purposes. Furthermore an influence of entrainment is apparent in the surface-layer structure with such an approach. The results compare well with alternative functions, but the scatter in observations is so large that we cannot determine the most favourable relationship.

In addition, we consider the behaviour of the non-dimensional surface sensible heat flux, J , for different flux–profile relations for large $-z/L$. These behave clearly differently: the function proposed by DeBruin (1999) reaches a constant value of 1.7 in the limit $-z/L \rightarrow \infty$. The Wilson (2001) function reaches 0.8 in this limit while the relation from Businger–Dyer grows to infinity. The observations from CASES-99 support the Wilson (2001) function.

We illustrated that the boundary-layer depth and the entrainment flux may play an important role in surface-layer scaling. However, the observations show a large scatter and therefore need special attention in the future; they should include the CBL depth, surface and entrainment fluxes, profiles and additional data to close the boundary-layer budgets and the surface energy budget. Not only potential temperature and humidity should be studied, but also CO_2 , which is an important trace gas. In addition, when new data become available with good closure of the surface energy balance, it is recommended to verify Equations (3) and (4).

Acknowledgements

The authors want to thank Fred C. Bosveld, Henk Klein Baltink and Sander Tijm from the Royal Netherlands Meteorological Institute (KNMI) for making available the Cabauw dataset. We also want to thank our colleagues Jordi Vilà-Guerau de Arellano for his advices, as well as Oscar Hartogensis and Bas van de Wiel for acquiring the CASES-99 dataset. We also wish to thank three unknown referees for their constructive comments.

Appendix A. Fluxes and gradients in the CBL

In steady state conditions it can be shown that (CH98; Frech and Mahrt, 1995; Holtslag, 1998):

$$\overline{w\chi} = -K \frac{\partial \overline{X}}{\partial z} + \overline{w\chi}_{\text{NL}} \quad (\text{A1})$$

is a good description of the fluxes and vertical gradients in a CBL. Here K is the eddy diffusivity and

$$\overline{w\chi}_{\text{NL}} = \gamma L_1 \left(\frac{w_*}{\sigma_w} \right) \frac{w_* \chi_*}{h} \quad (\text{A2})$$

is the non-local flux term; L_1 is a length scale defined by

$$L_1 = K / \sigma_w c_k. \quad (\text{A3})$$

In a quasi-stationary state we may also assume linear profiles of $\overline{w\chi}$ as a function of the normalised boundary-layer depth h (see Tennekes and Driedonks, 1981):

$$\overline{w\chi} = \overline{w\chi}_0 \left(1 - \frac{z}{h} \right) + \overline{w\chi}_e \frac{z}{h}, \quad (\text{A4})$$

where $\overline{w\chi}_0$ and $\overline{w\chi}_e$ are the surface flux and entrainment flux respectively. Subsequently the mean temperature gradient can be derived when the eddy diffusivity K and the vertical velocity variance in a CBL are represented by (Holtslag and Moeng, 1991)

$$K = w_* h \left(\frac{z}{h} \right)^{4/3} \left(1 - \frac{z}{h} \right)^2, \quad (\text{A5})$$

$$\sigma_w^3 = 1.2 w_*^3 \left(\frac{z}{h} \right) \left(1 - \beta \frac{z}{h} \right)^{3/2}. \quad (\text{A6})$$

The entrainment flux $\overline{w\theta}_e$ in Equation (3) can now be estimated for potential temperature by applying

$$\overline{w\theta}_e = \alpha \overline{w\theta}_0. \quad (\text{A7})$$

Then, the scalar gradient in a CBL can be derived resulting in Equation (3). The required parameters are taken from CH98, e.g. $\gamma = 1.5$ and $c_k = 0.3$. Finally $\beta = 0.9$ (Holtslag and Moeng, 1991).

References

- Akima, H.: 1970, 'A New Method of Interpolation and Smooth Curve Fitting Based on Local Procedures', *J. Assoc. Comp. Mach.* **17**, 589–602.
- Beljaars, A. C.: 1995, 'The Parameterization of Surface Fluxes in Large Scale Models Under Free Convection', *Quart. J. Roy. Meteorol. Soc.* **121**, 255–270.
- Businger, J. A.: 1973, 'A Note on Free Convection', *Boundary-Layer Meteorol.* **4**, 323–326.
- Businger, J. A.: 1988, 'A Note on the Businger–Dyer Profiles', *Boundary-Layer Meteorol.* **42**, 145–151.
- Businger, J. A., Wyngaard, J. C., Izumi, Y. and Bradly, E. F.: 1971, 'Flux Profile Relationships in the Atmospheric Surface Layer', *J. Atmos. Sci.* **28**, 181–189.
- Cuijpers, J. W. M. and Holtslag, A. A. M.: 1998, 'Impact of Skewness and Nonlocal Effects on Scalar and Buoyancy Fluxes in Convective Boundary Layers', *J. Atmos. Sci.* **55**, 151–161.

- DeBruin, H. A. R.: 1999, 'A Note on Businger's Derivation of Nondimensional Wind and Temperature Profiles Under Unstable Conditions', *J. Appl. Meteorol.* **38**, 626–628.
- DeBruin, H. A. R. and Holtslag, A. A. M.: 1982, 'A Simple Parameterization of the Surface Fluxes of Sensible and Latent Heat during Daytime Compared with the Penman–Monteith Concept', *J. Appl. Meteorol.* **21**, 1610–1621.
- Dyer, A. J.: 1974, 'A Review of Flux–Profile Relationships', *Boundary-Layer Meteorol.* **7**, 363–372.
- Frech, M. and Mahrt, L.: 1995, 'A Two-scale Mixing Formulations for the Atmospheric Boundary Layer', *Boundary-Layer Meteorol.* **73**, 91–104.
- Fleagle, R. G. and Businger, J. A.: 1980, *An Introduction to Atmospheric Physics*, 2nd edn, Academic Press, New York, 432 pp.
- Frenzen, P. and Vogel, A. G.: 2001, 'Further Studies of Atmospheric Turbulence in Layers near the Surface: Scaling the TKE Budget above the Roughness Sublayer', *Boundary-Layer Meteorol.* **99**, 173–206.
- Halldin, S., Bergström, H., Gustafsson, D., Dahlgren, L., Hjelma, P., Lundina, L.-C., Mellander, P.-E., Norda, T., Jansson, P.-E., Seibert, J., Stähli, M., Szilágyi Kishné, A., Smedman, A.-S.: 1999, 'Continuous Long-term Measurements of Soil-Plant-Atmosphere Variables at an Agricultural site', *Agric. Forest. Meteorol.* **98–99**, 75–102.
- Högström, U.: 1988, 'Non Dimensional Wind and Temperature Profiles in the Atmospheric Surface Layer: a Re-evaluation', *Boundary-Layer Meteorol.* **42**, 55–78.
- Holtslag, A. A. M.: 1998, 'Modeling of Atmospheric Boundary Layers, in *Clear and Cloudy Boundary Layers*', in A. A. M. Holtslag and P. G. Duynkerke (eds), Royal Netherlands Academy of Arts and Sciences, Amsterdam, 372 pp.
- Holtslag, A. A. M. and Nieuwstadt, F. T. M.: 1986, 'Scaling the Atmospheric Boundary Layer', *Boundary-Layer Meteorol.* **36**, 201–209.
- Holtslag, A. A. M. and Moeng, C. H.: 1991, 'Eddy Diffusivity and Countergradient Transport in the Convective Atmospheric Boundary-Layer', *J. Atmos. Sci.* **48**, 1690–1698.
- Johansson, C., Smedman, A. S., Högström U., Brasseur, J. G., and Khanna, S.: 2001, 'Critical test of the Validity of Monin–Obukhov Similarity During Convective Conditions', *J. Atmos. Sci.* **58**, 1549–1566.
- Kader, B. A. and Yaglom, A. M.: 1990, 'Mean Fields and Fluctuation Moments in Unstably Stratified Turbulent Boundary Layers', *J. Fluid Mech.* **212**, 637–662.
- Lumley, J. I. and Panofsky, H. A.: 1964, *The Structure of Atmospheric Turbulence*, Interscience Publishers, A division of John Wiley and Sons, New York and London, 239 pp.
- Mahrt, L., Vickers, D., Sun, J., Jensen, N. O., Jorgenson, H., Pardyjak, E., and Fernando, H.: 2001, 'Determination of the Surface Drag Coefficient', *Boundary-Layer Meteorol.* **99**, 249–276.
- Moeng, C. H. and Wyngaard, J. C.: 1989, 'Evaluation of Turbulent Transport and Dissipation Closures in Second-order Modeling', *J. Atmos. Sci.* **46**, 2311–2330.
- Monin, A.S. and Yaglom, A. M.: 1981: *Statistical Fluid Mechanics: Mechanics of Turbulence*, Part I, The MIT press, 900 pp.
- Oncley, S. P., Friehe, C. A., Larue, J. C., Businger, J. A., Itsweire, E. C. and Chang, S. S.: 1996, 'Surface-layer Fluxes, Profiles, and Turbulence Measurements over Uniform Terrain under near Neutral Conditions', *J. Atmos. Sci.* **53**, 1029–1044.
- Oncley, S. P., Foken, T., Vogt, R., Bernhofer, C., Kohsiek, W., Liu, H., Pitacco, A., Grantz, D., Riberio, L. and Weidinger, T.: 2002, 'The Energy Balance Experiment EBEX-2000', in *15th Symposium on Boundary-layer and Turbulence*, Wageningen, The Netherlands, 15–19 August 2002, American Meteorological Society, Boston, pp. 1–4.

- Panofsky, H. A., Tennekes, H., Lenschow, D. H. and Wyngaard, J. C.: 1977, 'The Characteristics of Turbulent Velocity Components in the Surface Layer under Convective Conditions', *Boundary-Layer Meteorol.* **11**, 355–361.
- Poulos, G. S. et al.: 2002, CASES-99: 'A comprehensive Investigation of the Stable Nocturnal Boundary Layer', *Bull. Amer. Meteorol. Soc.* **83**, 555–581.
- Rao, K. G.: 2004, 'Estimation of the Exchange Coefficient of Heat During Low Wind Convection Conditions', *Boundary-Layer Meteorol.* **111**, 247–273.
- Schumann, U.: 1988, 'Minimum Friction Velocity and Heat Transfer in the Rough Surface Layer of a Convective Boundary Layer', *Boundary-Layer Meteorol.* **44**, 311–326.
- Stull, R. B.: 1988, *An Introduction to Boundary-layer Meteorology*, Kluwer Academic Publishers, Dordrecht, 666 pp.
- Tennekes, H. and Driedonks, A. G. M.: 1981, 'Basic Entrainment Equations for the Atmospheric Boundary Layer', *Boundary-Layer Meteorol.* **20**, 515–531.
- Turner, J.S.: 1979, *Buoyancy Effects in Fluids*, Cambridge University Press, Cambridge, paperback edition, 368 pp.
- Van Ulden, A. P. and Wieringa, J.: 1996, 'Atmospheric Boundary Layer Research at Cabauw', *Boundary-Layer Meteorol.* **78**, 36–69.
- Wilson, D. K.: 2001, 'An Alternative Function for the Wind and Temperature Gradients in Unstable Surface Layers', *Boundary-Layer Meteorol.* **99**, 151–158.
- Wyngaard, J. C.: 1973, 'On Surface Layer Turbulence', in D. A. Haugen, (ed.), *Workshop on Micrometeorology*, American Meteorological Society, pp. 101–149.